Journal of Psychiatric Research 113 (2019) 108–116

Contents lists available at ScienceDirect

Journal of Psychiatric Research

journal homepage: www.elsevier.com/locate/jpsychires

Distinct resting state functional connectivity abnormalities in hoarding disorder and major depressive disorder

Hannah C. Levy[a,*], Michael C. Stevens[b,c], David C. Glahn[b,c], Krishna Pancholi[b], David F. Tolin[a,c]

[a] Anxiety Disorders Center, Institute of Living/Hartford Hospital, 200 Retreat Avenue, Hartford, CT, 06106, USA
[b] Olin Neuropsychiatry Research Center, Institute of Living/Hartford Hospital, 400 Washington Street, Hartford, CT, 06106, USA
[c] Department of Psychiatry, Yale University School of Medicine, 300 George Street, New Haven, CT, 06511, USA

ARTICLE INFO

Keywords:
fMRI
Hoarding disorder
Depression
Resting state

ABSTRACT

Emerging research suggests that hoarding disorder (HD) is associated with abnormal hemodynamic activity in frontal brain regions. Prior studies have not examined intrinsic network connectivity in HD during unstructured "resting state" fMRI. Furthermore, it remains unclear whether previously observed HD abnormalities might be better explained by the presence of other disorders frequently comorbid with HD, such as major depressive disorder (MDD). The current study compared resting state functional connectivity in HD-only patients (n = 17), MDD-only patients (n = 8), patients with co-occurring HD and MDD (n = 10), and healthy control participants (n = 18). Using independent component analysis, we found that HD-only patients exhibited lower functional connectivity in a "task positive" cognitive control network, compared to the other three groups. The HD group also had greater connectivity in regions of the "task negative" default mode network than did the other groups. Findings suggest that HD is associated with a unique neurobiological profile, and are discussed in terms of recent neurological and neuropsychological findings and models in HD and related disorders.

Hoarding disorder (HD) is characterized by difficulty discarding personal possessions regardless of their value, leading to excessive clutter in the home and other areas (American Psychiatric Association, 2013). Although no formal neurobiological model of HD yet exists, emerging neuroimaging research suggests abnormal activation in frontal brain regions associated with decision making and other executive functions. Functional magnetic resonance imaging (fMRI) studies have found neural activation differences in the anterior cingulate cortex (ACC), bilateral insula, and bilateral thalamus during real-time or imagined discarding in individuals with HD compared to those without HD (Boschen, Neumann and Waters, 2009; Tolin, Kiehl, Worhunsky, Book and Maltby, 2009; Tolin et al., 2012). Importantly, these differences were correlated with HD symptom severity, and were not attributable to obsessive-compulsive disorder (OCD) or depression severity (Tolin et al., 2012). In a related study, Tolin, Witt, and Stevens (2014) examined brain activation among HD patients, OCD patients, and HCs during a response inhibition (Go/No Go) task. When HD patients successfully inhibited their responses (correct rejects), they showed greater activation in right precental gyrus compared to OCD patients and less activation in left middle frontal gyrus compared to controls. By contrast, no group differences in neural activation were noted during errors of commission (unsuccessful response inhibition). Consistent with these results, Hough et al. (2016) recently reported increased activation in frontal regions (ACC and right dorsolateral prefrontal cortex) during response inhibition in HD participants compared to participants with OCD and healthy controls.

Taken together, these emerging results suggest that HD is neurobiologically distinct from OCD, and is characterized by discrete abnormalities in frontal brain regions. As a complement to task-based fMRI, it is possible to examine neural activity during a resting state when participants are not engaged in directed cognitive activity (van den Heuvel and Hulshoff Pol, 2010). Although Saxena et al. (2004) described resting-state brain metabolic abnormalities in OCD patients with prominent hoarding symptoms, no studies have used resting-state fMRI in HD patients in order to gain insight into intrinsic network functional connectivity across distributed systems. Cross-correlation or comparable statistical approaches can quantify the degree to which distributed brain regions co-engage to form networks, across which it is presumed that information processing frequently occurs. Such research has shown that a network of brain regions (the default mode network, DMN), comprising the posterior cingulate (PCC), precuneus, medial prefrontal cortex (MPFC), and posterior temporal cortical areas, typically have high activity during unstructured rest and internally-focused cognitive activities (e.g., mind wandering; Christoff, Gordon,

* Corresponding author.
E-mail address: hannah.levy@hhchealth.org (H.C. Levy).

https://doi.org/10.1016/j.jpsychires.2019.03.022
Received 27 August 2018; Received in revised form 27 February 2019; Accepted 21 March 2019

Smallwood, Smith and Schooler, 2009; Raichle et al., 2001), but decrease during task performance. This "task negative" network is complemented by what Raichle originally dubbed "task positive" brain regions largely in prefrontal and parietal cortices that form networks engaged by a wide variety of cognitive tasks (Raichle, 2015). To our knowledge, no prior studies have investigated neural activity in the "task negative" network during rest in patients with HD. However, it is reasonable to hypothesize that connectivity in both the "task negative" and "task positive" systems may be impaired in HD given growing evidence of neural activation abnormalities in HD patients as described above.

HD somewhat resembles other neuropsychiatric disorders that are characterized by similar cognitive deficits such as major depressive disorder (MDD), attention-deficit/hyperactivity disorder (ADHD), and OCD. There is ample evidence that these other disorders show abnormal connectivity during cognitive and executive functioning tasks (Bush, 2010; Castellanos et al., 2008; Nakao et al., 2005), giving rise to the possibility that HD might show comparable network connectivity abnormalities. A useful question to frame an HD resting state functional connectivity study is to ask whether HD shares the same brain connectivity abnormalities with other disorders most frequently found to be comorbid with HD, or whether it has a distinct profile of brain dysfunction. In particular, HD and MDD most often co-occur, with more than 50% of HD patients meeting diagnostic criteria for MDD in comparison to only 20% meeting criteria for OCD (Frost, Steketee and Tolin, 2011). Reviews of resting-state fMRI studies in MDD have found abnormal resting state functional connectivity in medial prefrontal cortex (MPFC), posterior cingulate cortex (PCC), precuneus, and medial, lateral, and inferior parietal cortices (Wang, Hermens, Hickie and Lagopoulos, 2012; Zhong, Pu and Yao, 2016). Given the comorbidity between HD and MDD and evidence for some similar cognitive deficits (e.g., difficulty concentrating; Marazziti, Consoli, Picchetti, Carlini and Faravelli, 2010), it is important to ensure that any intrinsic network connectivity abnormalities that might be observed in HD cannot be attributed to MDD. As such, MDD is a highly suitable comparison disorder for clarifying whether HD has a distinct neurobiological profile that is characterized by unique brain dysfunction.

The purpose of the current study was to compare resting state brain function in the task-negative default mode network and the task-positive cognitive control network in HD-only patients ("HD group"), MDD-only patients ("MDD group"), patients with co-occurring HD and MDD ("HD + MDD group"), and healthy controls ("HC group"). Our primary goal was to identify potential HD-specific connectivity abnormalities in order to further expand and detail a nascent neurobiological model of HD and to differentiate any observed abnormalities from MDD. Given the strong evidence that HD is neurobiologically distinct from OCD as reviewed above, we elected not to include an OCD comparison sample. Given that this is the first study of resting state functional connectivity in HD, our exploratory aims employed a statistical inference framework capable of identifying group differences across the entire brain while adequately controlling Type I error. We hypothesized that HD patients would exhibit connectivity abnormalities in both task-positive and task-negative network regions, and that these would differ characteristically from connectivity profiles found in MDD.

1. Materials and methods

1.1. Participants

fMRI data were collected from an HD group ($n = 17$), an MDD group ($n = 8$), an HD + MDD group ($n = 10$), and an HC group ($n = 18$) as part of two research studies, the first examining brain function in HD (Tolin et al., 2012; Tolin et al., 2014) and the second investigating biomarkers of mood disorders (unpublished). Participants were enrolled from October 2007 through October 2013. See Table 1 for demographic and clinical characteristics of the sample. As can be seen in the table, groups did not differ with respect to age, sex, race, ethnicity, or education level. Relative to the HD-only group (35%), a greater proportion of patients in the MDD (100%) and HD + MDD (90%) groups were taking psychiatric medications. Fifty-three percent of the HD-only group and 70% of the HD + MDD group had a comorbid anxiety disorder. There were no patients with comorbid anxiety disorders in the MDD-only group. There were also no patients with comorbid OCD across the three clinical groups.

The HD and HD + MDD group inclusion criterion was having a primary diagnosis of HD of at least moderate severity as assessed by the *Hoarding Rating Scale-Interview* (see below). For the HD + MDD group, the comorbid depressive disorder could be of any severity as long as it was severe enough to be diagnosable. The MDD group inclusion criterion was having a diagnosis of MDD as determined by the Structured Clinical Interview for DSM-IV-TR Axis I Disorders-Patient Edition (SCID I/P; First, Spitzer, Gibbon and Williams, 1995). Exclusion criteria for the HD, HD + MDD, and MDD clinical groups were a history of psychotic disorder or neurologic disorder, current substance use disorder, and current active suicidal ideation. Participants in the HC group had no current or past psychiatric disorder, no history of neurologic disorder, and were not taking psychiatric medications. Individuals who were deemed unsuitable for fMRI (e.g., those with metal implants) were excluded from all groups.

1.2. Measures

The following interviews were conducted by trained postdoctoral fellows or postgraduate research assistants.

For the HD and HD + MDD groups, the *Hoarding Rating Scale-Interview* (HRS-I; Tolin, Frost and Steketee, 2010) was used to determine HD diagnosis. The HRS-I is a clinician-administered semi-structured interview that assesses the severity of clutter, difficulty discarding, and compulsive acquiring, as well as distress and impairment associated with these symptoms.

For the HD, HD + MDD, and HC groups, all other psychiatric diagnoses, including MDD, were assessed using the *Anxiety Disorders Interview Schedule for DSM-IV* (ADIS-IV; Di Nardo, Brown and Barlow, 1994), a clinician-administered semi-structured diagnostic interview. The ADIS-IV assesses current and lifetime anxiety, mood, substance use, somatoform, and psychotic disorders. Clinicians rate the severity of each diagnosis on a 0 (*Complete absence of symptoms*) to 8 (*Severe symptoms*) scale; a severity rating of 4 or higher indicates a diagnosable disorder. To be included in the HD + MDD group, patients had to have diagnoses of HD and MDD as determined by the HRS-I and ADIS-IV.

Because the MDD group participants were recruited from a different study, they completed a different assessment protocol. For these patients, MDD and comorbid conditions were assessed with the SCID I/P (First et al., 1995), a semi-structured diagnostic interview that assesses psychiatric disorders based on the DSM-IV criteria (American Psychiatric Association, 1994). Because the SCID I/P does not assess hoarding, participants in the MDD group were not specifically evaluated for the presence or absence of HD symptoms.

All participants also completed the *Hamilton Depression Rating Scale* (HAM-D; Hamilton, 1960). The HAM-D is a 17-item clinician-administered interview that assesses depression severity over the past week. To be eligible for the MDD group, patients had to have a score of 14 or greater on the HAM-D, indicating at least moderate depression severity.

1.3. Procedure

The study was carried out in accordance with the latest version of the Declaration of Helsinki and approved and monitored by the Hartford Hospital Institutional Review Board. All participants signed an informed consent document that was explained carefully, and were given the opportunity to ask questions. The investigator affirmed that participants were capable of providing informed consent. After

Table 1
Sample characteristics.

	HD	MDD	HD + MDD	HC	F or X^2 (p)
Age, *M* (*SD*)	47.24 (10.17)	51.13 (5.82)	49.40 (7.23)	46.28 (8.44)	0.73 (.537)
Female sex, % (*n*)	58.8 (10)	62.5 (5)	90.0 (9)	50.0 (9)	4.51 (.211)
Race, % (*n*)					10.71 (.098)
Black	0.0 (0)	12.5 (1)	0.0 (0)	27.8 (5)	
White	94.1 (16)	87.5 (7)	100 (10)	66.7 (12)	
More than one race	5.9 (1)	0.0 (0)	0.0 (0)	0.0 (0)	
Unknown/Unreported	5.9 (1)	0.0 (0)	0.0 (0)	5.6 (1)	
Ethnicity, % (*n*)					1.14 (.768)
Hispanic/Latino	5.9 (1)	0.0 (0)	1.0 (0)	5.6 (1)	
Not Hispanic/Latino	88.2 (15)	100 (8)	100 (10)	88.9 (16)	
Unknown/Unreported	5.9 (1)	0.0 (0)	0.0 (0)	5.6 (1)	
Highest education attained					11.13 (.743)
Doctorate	17.6 (3)	0.0 (0)	20.0 (2)	0.0 (0)	
Master's degree	5.9 (1)	12.5 (1)	10.0 (1)	11.1 (2)	
Some graduate school	23.5 (4)	12.5 (1)	0.0 (0)	16.7 (3)	
Bachelor's degree	35.3 (6)	37.5 (3)	40.0 (4)	16.7 (3)	
Some college/Associate's	11.8 (2)	25.0 (2)	30.0 (3)	16.7 (3)	
High school diploma	5.9 (1)	12.5 (1)	0.0 (0)	0.0 (0)	
Unknown	0.0 (0)	0.0 (0)	0.0 (0)	38.9 (7)	
On psychiatric medications, % (*n*)	$35.3\ (6)_a$	$100\ (8)_b$	$90.0\ (9)_{b,\ c}$	–	13.77 (.001)
HRS-I, *M* (*SD*)	23.65_a (3.46)	–	$28.22\ (5.38)_b$	–	6.98 (.014)
HAM-D, *M* (*SD*)	$4.94\ (3.98)_a$	$20.38\ (4.17)_b$	$11.00\ (3.40)_c$	$0.47\ (0.83)_d$	72.17 (< .001)
Comorbid anxiety, % (*n*)	52.9 (9)	0 (0)	70.0 (7)	–	1.98 (.160)
Comorbid PTSD, % (*n*)	0 (0)	12.5 (1)	10.0 (1)	–	0.03 (.867)

Note. HD = Hoarding disorder. MDD = Major depressive disorder. HC = Healthy control. HRS = Hoarding Rating Scale-Interview. HAM-D = Hamilton Depression Rating Scale. PTSD = Posttraumatic stress disorder. Comorbid anxiety refers to DSM-5 anxiety disorder diagnoses. Values that do not share subscripts are significantly different from each other, $p < .05$.

providing written informed consent, participants completed the ADIS-IV and HRS-I (HD, HD + MDD, and HC groups) or the SCID (MDD group) with a trained clinician. They then completed the fMRI protocol. During the fMRI session, participants were given time to habituate to the scanner environment before fMRI data collection. For the resting-state scan, participants were asked to fixate on a black screen with a small white cross in the center. They were asked to remain awake and alert with their eyes open during the entire scan, which lasted for 5 min and 15 s.

1.4. Imaging parameters and processing

All MRI data were collected using a 3.0 T S Allegra MRI scanner (Erlangen, Germany) at the Olin Neuropsychiatry Research Center, Institute of Living/Hartford Hospital. fMRI data were acquired using a gradient-echo echo-planar imaging (EPI) pulse sequence: repetition time (TR) = 1500 msec, echo time (TE) = 28 msec, flip angle = 65°, field of view = 24 × 24 cm, acquisition matrix = 64 × 64, A » P phase encoding, voxel size = 3.4 × 3.4 mm, slice thickness = 5 mm, number of slices = 29 (acquired sequentially). Gradient echo fieldmaps: TR = 580 msec, TE = 7 msec, flip angle = 90°, matrix = 128 × 128, A » P phase encoding, 3 mm slice thickness. MPRAGE T1-weighted images of brain structure: TR = 2500 msec, TE = 2.74 msec, flip angle = 8°, matrix = 256 × 208, 1 mm slice thickness.

Each fMRI timeseries was realigned to the mid-series volume (Jenkinson, Bannister, Brady and Smith, 2002), corrected for slice-timing acquisition differences (Jenkinson, Beckmann, Behrens, Woolrich and Smith, 2012) and spatial distortions due to in-homogeneity removed using fieldmap-based unwarping (Jenkinson, 2003). Head motion was infrequent, as average framewise displacement (Power, Barnes, Snyder, Schlaggar and Petersen, 2012) was only 0.25 mm for the sample. Neither mean framewise displacement ($F_{3,49} = 0.535$, $p = .661$) nor the number of head movements > 0.5 mm in each timeseries ($F_{3,49} = 0.353$, $p = .787$) differed across the four study groups. The influence of micromovements and any infrequent signal spikes were removed using AFNI 3dDespike (Cox, 1996). Volumes were automatically reoriented to stereotactic space using 3-parameter rigid body realignment. An example fMRI volume was co-registered to the MPRAGE high-resolution brain structure scan, then spatial normalization parameters mapping the T1 to MNI atlas space were applied to each fMRI volume. Each image of the resulting timeseries was spatially smoothed with a 6 mm FWHM Gaussian kernel.

1.5. Functional connectivity independent component analysis (ICA)

ICA is a whole brain, data-driven multivariate analysis method that identifies distinct groups of brain regions with the same temporal pattern of hemodynamic signal change. Analysis included intensity normalization, two principal component analyses (PCA) concatenated data reduction stages (Calhoun, Adali, Pearlson and Pekar, 2001; Schmithorst and Holland, 2004), and estimation of independent components using an algorithm that minimizes the mutual information of the network outputs (Bell and Sejnowski, 1995). The final ICA rotation was performed on the group of participants' aggregate data and produced spatial maps and timecourses that represented both the spatial and temporal characteristics of each component's "functionally-connected network." This group solution was used to back-reconstruct single-subject time courses and spatial maps from the raw data using methods that accurately preserved participant-to-participant variability (i.e., GICA3; Erhardt et al., 2010). The ICA methods are available in a Group ICA of fMRI Toolbox (GIFT v1.3 h) implemented in Matlab (http://icatb.sourceforge.net). Data dimensionality (number of components) was estimated using the minimum description length (MDL) criteria tool in GIFT, which suggested that 21 components were present in the data (Li, Adali and Calhoun, 2007). ICA solution reliability was assessed using ICASSO (http://www.cis.hut.fi/projects/ica/icasso) across 100 separate FastICA estimations, where Iq coefficients for the components ranged from 0.966 to 0.986. We correlated component maps with an *a priori* grey matter mask and rejected from further consideration any component where the R^2 was less than 0.15 indicating the voxels in the spatial map were a poor match to normal grey matter. As an additional check for component validity, we examined the fractional amplitude of low-frequency fluctuations (fALFF) across each component's timecourse. Non-artifactual ICA-identified signals

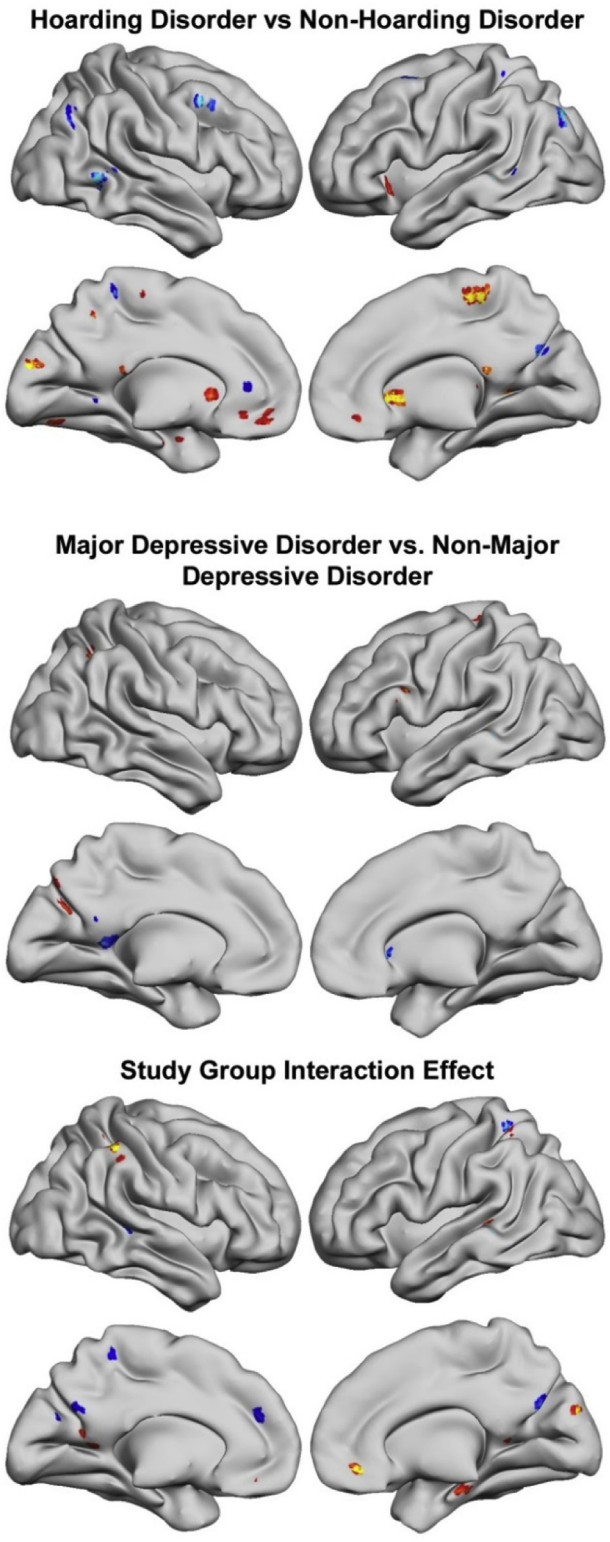

Fig. 1. For main effects of Hoarding or Major Depressive Disorder diagnosis (top and middle), red-yellow represents less functional connectivity in the each diagnostic group compared to participants without the diagnosis, while blue-scale represents more connectivity, as listed in Tables 1 and 2 For interaction effects (bottom), red-yellow and blue-scale colors were arbitrarily chosen to represent the negative and positive interaction effects of the two diagnostic groups (Table 3). (For interpretation of the references to colour in this figure legend, the reader is referred to the web version of this article.)

typically have a greater fALFF values at the lowest frequency bins. We rejected components where the ratio of low/high bins was less than 3.0.

1.6. Group hypothesis-testing

Of the 11 components that remained after quality control and inspection for artifacts, one clearly depicted both the default mode network and the task-positive network of various brain regions often engaged during cognitively demanding tasks in the same spatial map (see Fig. 1). Although data-driven ICA can sometimes separate task-negative and task-positive systems, it also is common to see them represented together as a single source (i.e., the co-occurrence reflects frequently described anti-correlation of these systems). The default mode was most prominent in this component, with brain regions typically seen engaged for cognitive control being co-engaged to a lesser extent, yet anti-correlated to this dominant focus. Specifically, these control regions included the frontal eye fields anterior to and including precentral gyri bilaterally, as well as proximal supplemental motor area cortex on both the lateral and medial surfaces of the brain, cingulate gyrus (BA 24), and bilateral caudate. Inspection of these regions (see Supplemental Figure 1) shows a close correspondence with several bilateral middle and superior frontal gyri regions, left insula, and left putamen found to be anti-correlated with ventral precuneus in prior reports that used seed-voxel connectivity methods (Zhang and Li, 2012). Correlation of each network with intrinsic connectivity networks described in the Stanford FINDLAB's database (Shirer, Ryali, Rykhlevskaia, Menon and Greicius, 2012) found the strongest correlation to the Default Mode Network and Executive Control Networks. Though visual inspection shows the latter is not an exact fit, the component did contain elements of several different intrinsic connectivity networks linked to cognitive control (Laird et al., 2011; Power et al., 2011). Thus, this was the component we selected for subsequent hypothesis testing.

Each participant's spatial map was entered into an SPM12 factorial ANOVA, which contrasted HD and MDD diagnoses in a 2 (HD, yes or no) × 2 (MDD, yes or no) design. This procedure uses restricted maximum likelihood estimation to control properly-partitioned error variance across study groups for accurate inference of all main and interaction effects. Voxels in the map that have greater or lesser values for any factor in the model (e.g., HD diagnosis) can be interpreted as having stronger or weaker connectivity to the entire network. For instance, if a regional decrease in connectivity is found, that brain region has less connectivity. If this occurs in a task-negative default mode region, the most straightforward interpretation is that it is integrated with other default mode regions. However, it also is accurate to extend the context with the realization that it is probably less anti-correlated with the task-positive regions as well. Multiple comparisons controlling for searching the entire brain volume were implemented using a clusterwise inference framework (Forman et al., 1995) requiring both a cluster-determining threshold (CDT) of $p < .005$ (Cox, Chen, Glen, Reynolds and Taylor, 2017) and extent thresholds to be surpassed for results to be considered significant at a "whole brain" $p < .05$ level of significance. To address recent concerns that this inference method can inflate false positive rates (Eklund, Nichols and Knutsson, 2016), we used updated AFNI code that corrected for inaccurate search volume space "edge effects" and a new method to estimate noise smoothness with a non-Gaussian spatial autocorrelation function (ACF). ACF parameters were determined using AFNI's 3dFWHMx function, using input from SPM's estimates of the smoothness of the noise, not the statistical images themselves. A cluster extent threshold of 30 voxels (810 mm^3) corresponded to $p < .05$ error rate control. To help judge the magnitude of the group differences that survived Type I error rate control, Cohen's *d* effect sizes for each reported finding are included. Anatomical localization was assisted using anatomical atlases (Eickhoff et al., 2005). To decompose the interaction effects, we conducted *post hoc* pairwise comparisons between groups. To control for multiple comparisons in these *post hoc* tests, we used a Bonferroni correction;

Table 2
Functional connectivity differences between participants with and without Hoarding Disorder. The table lists peak coordinates of group difference for clusters surpassing a cluster-determining threshold of 30 voxels (810 mm^3) corresponding to $p < .05$ "whole brain" correction for multiple comparisons. Cohen's *d* effect sizes for each region also are listed.

	Max Peak x, y, z	*t*	Cluster size (voxels)	*d*
Non-Hoarding Disorder > Hoarding Disorder				
Left insula	−26, 20, −2	3.72	49	1.06
Left superior orbital/rectal gyri	4, 40, −12	3.43	81	0.98
Right mid-cingulate gyrus	4, −32, 58	4.37	120	1.25
Right hippocampus (posterior)	12, −38, 14	3.41	74	0.97
Left fusiform gyrus/Cerebellum VI	−24, −78, −10	3.47	30	0.99
Left parahippocampal gyrus/amygdala	−23, −8, −24	3.48	30	0.99
Left cuneus	−6, −92, 20	4.82	51	1.38
Left caudate nucleus	−12, 14, 2	3.62	38	1.03
Right caudate nucleus	10, 14, 0	4.76	106	1.36
Left thalamus (temporal)	−4, −32, 16	4.05	56	1.16
Brainstem	2, −28, −36	5.13	88	1.47
Non-Hoarding Disorder < Hoarding Disorder				
Left middle frontal gyrus	−34, 6, 62	4.50	33	1.29
Left superior frontal gyrus	−22, 22, 44	3.38	30	0.97
Right middle frontal gyrus	40, 10, 44	4.29	55	1.23
Right insula/pars triangularis	36, 14, 18	4.21	75	1.20
Right superior middle frontal gryus	−6, 37, 6	3.45	55	0.99
Left precuneus	−14, −42, 64	3.75	55	1.07
Right precuneus	8, −70, 28	4.13	41	1.18
Left fusiform gyrus/hippocampus	−36, −46, 0	4.95	91	1.41
Left middle occipital gyrus	−34, −82, 36	4.76	49	1.36
Right middle occipital gyrus	38, −74 42	3.55	38	1.01
Left cerebellum	−8, −52, −2	3.51	30	1.00
Cerebellar vermis	4, −44, −18	3.92	32	1.12

0.05/6 (number of individual comparisons per ROI) = 0.008 α level.

2. Results

Table 2 lists brain regions for which there was a main effect of HD along with effect size estimates of the magnitude of group differences. Patients with HD had significantly lower functional connectivity in left superior orbital/rectal gyri, left and right caudate nuclei, left and right middle frontal gyrus, and left superior frontal gyrus. In our ICA solution, all these regions were functionally integrated into the task-positive cognitive control network, indicating lower connectivity between these regions and the "task positive" cognitive control component. The HD group also had lower connectivity in left cuneus, which is functionally connected to the cognitive control network, indicating lower connectivity with the "task positive" component. The HD group had significantly greater connectivity in left fusiform gyrus and precuneus, which are functionally connected to the default mode network, indicating greater connectivity with the "task negative" default mode network component.

Replicating extensive prior research, participants diagnosed with MDD differed from those without MDD, with large effect sizes (see Table 3). Patients with MDD showed significantly lower functional connectivity in nodes of the cognitive control network, i.e., left middle and inferior frontal gyri and angular gyrus. They also showed significantly higher connectivity in right caudate nucleus. Outside of the typical task-positive network, MDD also showed lower connectivity of left cuneus in the visual system. For the default mode network, the MDD group demonstrated higher precuneus connectivity.

Table 4 presents the interaction results and effect sizes that depict how HD-specific or MDD-specific connectivity findings were modified in the presence of the other diagnosis. For regions known to be engaged for cognitive control processes, there were negative interactions in rectal gyri, mid-cingulate, left superior parietal lobule, and right IPL/IPS. *Post hoc* testing showed that the strongest differences were for bilateral gyrus rectus, where the differences between HD-only and HC drove the interaction effect (see Fig. 2). For regions within or often found connected to the default mode network, there were positive interactions in left superior medial gyrus, precuneus, and cerebellum and negative interactions in left calcarine gyrus and right cuneus. *Post hoc* pairwise comparisons revealed significant differences between the MDD and HD + MDD groups in the superior medial frontal gyrus (see Fig. 3), but no other group differences between the HD + MDD group and the other groups were observed.

Table 3
Functional connectivity differences between participants with and without Major Depressive Disorder. The table lists peak coordinates of group difference for clusters surpassing a cluster-determining threshold of 30 voxels (810 mm^3) corresponding to $p < .05$ "whole brain" correction for multiple comparisons. Cohen's *d* effect sizes for each region also are listed.

	Max Peak x, y, z	*t*	Cluster size (voxels)	*d*
Non-Major Depressive Disorder > Major Depressive Disorder				
Left middle frontal gyrus	−26, 4, 54	4.09	36	1.17
Left inferior frontal gyrus (pars opercularis)	−50, 12, 24	3.96	31	1.13
Right angular gyrus	32, −60, 42	3.89	56	1.11
Left cuneus	−16, −70, 26	3.52	67	1.01
Left cerebellum (Crus 1)	−34, −60, −28	4.25	50	1.21
Non-Major Depressive Disorder < Major Depressive Disorder				
Left precuneus	−12, −48, 10	3.82	46	1.09
Right caudate nucleus/superior orbital gyrus	18, 20, 0	3.57	43	1.02

Table 4
Brain regions that showed an interaction between Hoarding Disorder and Major Depressive Disorder diagnoses. The table lists peak coordinates of group difference for clusters surpassing a cluster-determining threshold of 30 voxels (810 mm^3) corresponding to $p < .05$ "whole brain" correction for multiple comparisons. Cohen's *d* effect sizes for each region also are listed.

	Max Peak x, y, z	*t*	Cluster size (voxels)	*d*
Positive Interaction				
Left superior medial gyrus	−10, 42, 24	3.67	38	1.05
Left mid-cingulate gyrus	−20, −48, 60	4.41	73	1.26
Left/Right precuneus and left calcarine gyrus	4, −70, 28	3.26	63	0.93
Right superior temporal gyrus/hippocampus	40, −32, −2	3.80	92	1.09
Right cerebellum (VIII)	30, −48, −46	4.87	44	1.39
Negative Interaction				
Right/left rectal gyri	4, 40, −10	4.23	59	1.21
Left superior parietal lobule/postcentral gyrus	−38, −48, 62	3.73	39	1.07
Right supramarginal gyrus (IPL/IPS)	52, −40, 50	4.92	68	1.41
Left calcarine gyrus	−14, −58, 12	3.55	67	1.01
Right cuneus	12, −88, 24	3.72	41	1.06
Right parahippocampal gyrus	20, −16, −20	3.11	30	0.89

Note. IPL = Inferior parietal lobule. IPS = Superior parietal lobule.

3. Discussion

The purpose of this study was to examine resting-state functional connectivity in HD-only patients, MDD-only patients, co-occurring HD and MDD patients, and control participants without psychiatric disorders to answer two questions. First, we wanted to learn whether or not functional connectivity abnormalities could be detected in patients diagnosed with HD during unstructured rest (i.e., not in response to symptom provocation). The results clearly showed resting-state functional connectivity abnormalities in the HD group. If one considers all the HD connectivity abnormalities found across the whole brain, what emerges is a profile of diminished connectivity of several cingulo-opercular network regions involved in salience detection and error/conflict processing and of a handful of subcortical regions with functionally-specialized information processing that seems directly relevant to HD – decision-making/valuation (orbitofrontal; Tobia et al., 2014), remote memory (posterior hippocampus; Poppenk, Evensmoen, Moscovitch and Nadel, 2013), contextual memory representation (anterior parahippocampal gyrus; Baumann and Mattingley, 2016), and executive function as well as classification learning in the presence of rewarding reinforcers (caudate; Pauli, O'Reilly, Yarkoni and Wager, 2016; Seger and Cincotta, 2005). At the same time, HD showed over-connectivity relative to non-HD of numerous lateral surface prefrontal cortex regions, bilateral precuneus, visual cortex, and cerebellum.

On the one hand, these findings contribute to a growing literature on neurobiological mechanisms of HD that implicate the cognitive control network. For instance, in non-neuroimaging studies of cognitive abnormalities, patients with HD have shown deficits in tests of attention and task switching (Ayers et al., 2013), pointing to the potential importance of the cognitive control network in HD symptomatology. Also, prior analyses of fMRI data from the same sample of HD patients found activation abnormalities in cognitive control regions during both symptom provocation (Tolin et al., 2012) and successful response inhibition (Tolin et al., 2014). It is noteworthy that we found increased resting-state functional connectivity in some regions of the cognitive control network among HD patients, as during rest these regions are typically deactivated as the DMN is engaged (Ceko et al., 2015). This opens the door to considering models in which HD might be characterized by abnormal intrusion of cognitive processes into relaxed, non-task-driven states.

On the other hand, most of these HD connectivity abnormalities were not found in regions considered to be "core" and most-frequently studied cognitive control or DMN regions. A focus on the central regions of these networks highlights the over-connectivity of bilateral precuneus we found in HD. The precuneus is believed to be part of a hippocampal-parietal memory network reliably linked to recollection of previously studied information (Raichle, 2015). The precuneus and its inter-connected brain regions are involved in autobiographical recall, self-reflection, and consciousness (Cavanna and Trimble, 2006). It could be that over-connectivity in these regions may cause self-reflective thoughts to intrude into consciousness and lead to distractibility and difficulty sustaining attention, which are cognitive disturbances that have been observed in HD patients (Grisham, Brown, Savage, Steketee and Barlow, 2007; Hartl, Duffany, Allen, Steketee and Frost,

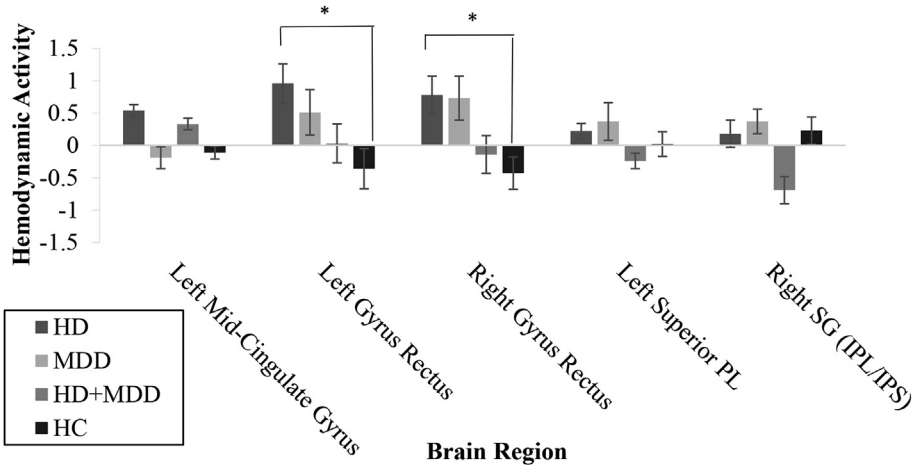

Fig. 2. Group differences in functional connectivity for regions in the cognitive control network depicted in the component. HD = Hoarding disorder group. MDD = Major depressive disorder group. HD + MDD = Comorbid hoarding disorder and major depressive disorder group. HC = Healthy control group. PL = Parietal lobule. SG = Supramarginal gyrus. IPL = Inferior parietal lobule. IPS = Superior parietal lobule. Error bars represent standard errors. *$p < .008$ (Bonferroni-corrected α).

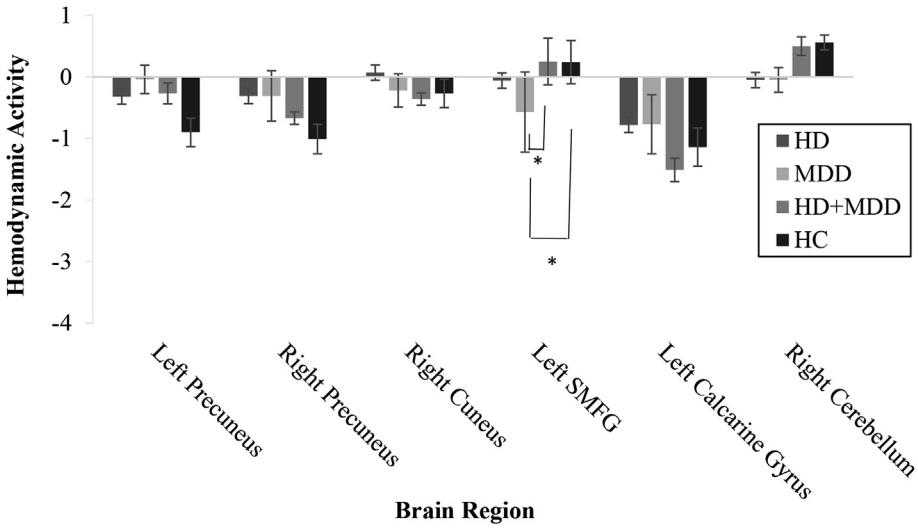

Fig. 3. Group differences in functional connectivity for regions in the default mode network depicted in the component. HD = Hoarding disorder group. MDD = Major depressive disorder group. HD + MDD = Comorbid hoarding disorder and major depressive disorder group. HC = Healthy control group. SMFG = Superior medial frontal gyrus. Error bars represent standard errors. *$p < .008$ (Bonferroni-corrected α).

2005; Tolin and Villavicencio, 2011). Of course, our interpretations of these findings are merely speculative and must be confirmed by future experimental manipulations.

Our second objective was to bolster the emerging theoretical model that HD neural abnormalities are distinctly different from those found in other frequently comorbid psychiatric disorders (i.e., MDD). We found several brain connectivity abnormalities in the HD group that were not observed in the other study groups, suggesting that HD is indeed characterized by a unique neurobiological profile. Similarly, the strongest differences from pairwise comparisons of the four study groups in cognitive control brain regions that had significant interactions between the HD and MDD factors primarily implicated differences between non-depressed HD and non-HD. The HD profile discussed above was qualitatively different from MDD connectivity abnormalities. Consistent with meta-analytic results of MDD resting state connectivity studies (Kaiser et al., 2016), we found reduced connectivity within the frontoparietal task-positive network in the MDD group. We also found decreased connectivity in the visual processing cortex in MDD patients, which has been highlighted in other meta-analytic reviews of MDD connectivity research (Zhong et al., 2016). The consistency of our MDD findings with those from prior studies increases confidence that our sampling and analytic approach produced credible results, despite a small sample size. It also is noteworthy that the effect sizes for the various MDD vs. non-MDD differences were of similar magnitude to the HD vs. non-HD differences (all were “large” Cohen's *d* effect sizes). We also found several interactions between HD and MDD, suggesting comorbid HD and MDD may be associated with unique brain abnormalities compared to having only one of these disorders. These interaction results not only identified several instances in which having both HD and MDD accentuated regional connectivity deficits in the default mode or closely connected regions with similar signal change profiles (e.g., right precuneus and visual cortex), but also some examples where comorbidity diminished or even normalized connectivity in the cognitive control network (e.g., gyrus rectus and caudate). Most *post hoc* comparisons between the HD + MDD group and the other groups were not statistically significant. Thus, simple conclusions about the neurobiology of HD + MDD patients seems premature, and further study is warranted to better understand the unique profiles of neural dysfunction in these patients.

The current study is not without limitations. First, this was a small sample with low cell sizes for certain groups (e.g., MDD group, $n = 8$). Because we chose to use statistical corrections for Type I error across the entire brain, it is likely that we could only detect the largest group differences in hemodynamic activity. However, given the novel nature of the study and the absence of highly theory-driven predictions, we think our approach was justified. Given the small sample size, we intended for this study to be a preliminary look at the potential differences between HD and MDD at the neurobiological level to guide future neurobiological model conceptualization and testing (Carter, Lesh and Barch, 2016). These results await replication and extension in larger and more diverse HD samples, and our work on this is underway. Second, both HD and MDD are heterogeneous disorders in terms of presenting symptoms, comorbidities, and current distress and impairment and it will be important to characterize these differences on the neural level. Third, although we carefully followed recent guidelines about proper clusterwise inference, it is worth noting that the extensive simulations that justified our choice of entry threshold were done on activation data, not functional connectivity. Due to its multivariate nature, ICA tends to produce data where the network structures are larger and more contiguous compared to regional activation studies. However, given how our analyses were designed to isolate localized differences in regional connectivity, the clusters had the same approximate size and thus this issue is unlikely to have impacted the inference framework we used. Fourth, MDD group participants were not specifically evaluated for HD, so we cannot rule out the possibility that some patients in this group met criteria for HD. However, given the small sample size of 8 patients in this group, this seems unlikely. Fifth, there were some differences with respect to psychiatric medications in the clinical groups, which may have affected our findings. We were missing data on education level for some of the HC participants ($n = 7$); we had complete education data for all clinical groups. Finally, although the ICA approach seemed an appropriate place to start for a small initial study such as this one, future connectivity research in HD might benefit from employing alternative techniques that can isolate various specific brain networks or examine specific connectivity-related features of those systems. Based on our findings and those of prior studies (Tolin et al., 2012), cognitive control-related networks should be a primary area of focus in future work. Recent research has already shown the topological and functional distinctiveness of many such intrinsic connectivity networks [e.g., cingulo-opercular, dorsal and ventral attention, and frontoparietal executive networks (Power et al., 2011)]. It will be important to establish whether or not there are links between network-related abnormalities in these various specific neural systems and HD-linked executive dysfunction that is emerging from our and other investigators’ research.

Acknowledgements

This work was supported by the National Institute of Mental Health (R01MH074934; PI: Tolin and R01MH080192; PI: Glahn) and Hartford

Hospital (Grant #126255; PI: Stevens).

Drs. Levy, Stevens, and Tolin contributed to manuscript preparation. Dr. Glahn contributed to data collection and manuscript editing. Ms. Pancholi assisted with data analyses. All authors have approved the article.

The authors wish to thank Anna Villavicencio, Ph.D., Melissa Norberg, Ph.D., and Nicholas Maltby, Ph.D. for their assistance with this project.

Appendix A. Supplementary data

Supplementary data to this article can be found online at https://doi.org/10.1016/j.jpsychires.2019.03.022.

Conflicts of interest

This work was supported by the National Institute of Mental Health (R01MH074934; PI: Tolin and R01MH080192; PI: Glahn) and Hartford Hospital (Grant #126255; PI: Stevens). Dr. Levy and Ms. Pancholi have no declarations of interest.

References

American Psychiatric Association, 1994. Diagnostic and Statistical Manual of Mental Disorders, fourth ed. (Washington, DC: Author).

American Psychiatric Association, 2013. Diagnostic and Statistical Manual of Mental Disorders, fifth ed. (Washington, DC).

Ayers, C.R., Wetherell, J.L., Schiehser, D., Almklov, E., Golshan, S., Saxena, S., 2013. Executive functioning in older adults with hoarding disorder. Int. J. Geriatr. Psychiatry 28 (11), 1175–1181. https://doi.org/10.1002/gps.3940.

Baumann, O., Mattingley, J.B., 2016. Functional organization of the parahippocampal cortex: dissociable roles for context representations and the perception of visual scenes. J. Neurosci. 36 (8), 2536–2542. https://doi.org/10.1523/JNEUROSCI.3368-15.2016.

Bell, A.J., Sejnowski, T.J., 1995. An information-maximization approach to blind separation and blind deconvolution. Neural Comput. 7 (6), 1129–1159.

Boschen, M.J., Neumann, D.L., Waters, A.M., 2009. Relapse of successfully treated anxiety and fear: theoretical issues and recommendations for clinical practice. Aust. N. Z. J. Psychiatr. 43 (2), 89–100 907921612 [pii] 1080/00048670802607154a.

Bush, G., 2010. Attention-deficit/hyperactivity disorder and attention networks. Neuropsychopharmacology 35 (1), 278–300. https://doi.org/10.1038/npp.2009.120.

Calhoun, V.D., Adali, T., Pearlson, G.D., Pekar, J.J., 2001. A method for making group inferences from functional MRI data using independent component analysis. Hum. Brain Mapp. 14 (3), 140–151.

Carter, C.S., Lesh, T.A., Barch, D.M., 2016. Thresholds, power, and sample sizes in clinical neuroimaging. Biol Psychiatry Cogn Neurosci Neuroimaging 1 (2), 99–100. https://doi.org/10.1016/j.bpsc.2016.01.005.

Castellanos, F.X., Margulies, D.S., Kelly, C., Uddin, L.Q., Ghaffari, M., Kirsch, A., ... Milham, M.P., 2008. Cingulate-precuneus interactions: a new locus of dysfunction in adult attention-deficit/hyperactivity disorder. Biol. Psychiatry 63 (3), 332–337. https://doi.org/10.1016/j.biopsych.2007.06.025.

Cavanna, A.E., Trimble, M.R., 2006. The precuneus: a review of its functional anatomy and behavioural correlates. Brain 129 (Pt 3), 564–583. https://doi.org/10.1093/brain/awl004.

Ceko, M., Gracely, J.L., Fitzcharles, M.A., Seminowicz, D.A., Schweinhardt, P., Bushnell, M.C., 2015. Is a responsive default mode network required for successful working memory task performance? J. Neurosci. 35 (33), 11595–11605. https://doi.org/10.1523/JNEUROSCI.0264-15.2015.

Christoff, K., Gordon, A.M., Smallwood, J., Smith, R., Schooler, J.W., 2009. Experience sampling during fMRI reveals default network and executive system contributions to mind wandering. Proc. Natl. Acad. Sci. U. S. A. 106 (21), 8719–8724. https://doi.org/10.1073/pnas.0900234106.

Cox, R.W., 1996. AFNI: software for analysis and visualization of functional magnetic resonance neuroimages. Comput. Biomed. Res. 29 (3), 162–173. https://doi.org/10.1006/cbmr.1996.0014.

Cox, R.W., Chen, G., Glen, D.R., Reynolds, R.C., Taylor, P.A., 2017. FMRI clustering in AFNI: false-positive rates redux. Brain Connect. 7 (3), 152–171. https://doi.org/10.1089/brain.2016.0475.

Di Nardo, P.A., Brown, T.A., Barlow, D.H., 1994. Anxiety Disorders Interview Schedule for DSM-IV: Lifetime Version (ADIS-IV-L). The Psychological Corporation, San Antonio, TX.

Eickhoff, S.B., Ktephan, K.E., Mohlberg, H., Grefkes, C., Fink, G.R., Amunts, K., Zilles, K., 2005. A new SPM toolbox for combining probabilistic cytoarchitectonic maps and functional imaging data. Neuroimage 25 (4), 1325–1335. https://doi.org/10.1016/j.neuroimage.2004.12.034.

Eklund, A., Nichols, T.E., Knutsson, H., 2016. Cluster failure: why fMRI inferences for spatial extent have inflated false-positive rates. Proc. Natl. Acad. Sci. U. S. A. 113 (28), 7900–7905. https://doi.org/10.1073/pnas.1602413113.

Erhardt, E.B., Rachakonda, S., Bedrick, E.J., Allen, E.A., Adlali, T., Calhoun, V.D., 2010. Comparison of multi-subject ICA methods for analysis of fMRI data. Hum. Brain Mapp. https://doi.org/10.1002/hbm.21170.

First, M.B., Spitzer, R.L., Gibbon, M., Williams, J.B.W., 1995. Structured Clinical Interview for DSM-IV Axis I Disorders-Patient Edition (SCID I/P, Version 2.0). Biometrics Research Department, New York.

Forman, S.D., Cohen, J.D., Fitzgerald, M., Eddy, W.F., Mintun, M.A., Noll, D.C., 1995. Improved assessment of significant activation in functional magnetic resonance imaging (fMRI): use of a cluster-size threshold. Magn. Reson. Med. 33 (5), 636–647. https://doi.org/10.1002/mrm.1910330508.

Frost, R.O., Steketee, G., Tolin, D.F., 2011. Comorbidity in hoarding disorder. Depress. Anxiety 28 (10), 876–884. https://doi.org/10.1002/da.20861.

Grisham, J.R., Brown, T.A., Savage, C.R., Steketee, G., Barlow, D.H., 2007. Neuropsychological impairment associated with compulsive hoarding. Behav. Res. Ther. 45, 1471–1483. https://doi.org/10.1016/j.brat.2006.12.008.

Hamilton, M., 1960. A rating scale for depression. J. Neurol. Neurosurg. Psychiatry 23, 56–62. https://doi.org/10.1136/jnnp.23.1.56.

Hartl, T.L., Duffany, S.R., Allen, G.J., Steketee, G., Frost, R.O., 2005. Relationships among compulsive hoarding, trauma, and attention-deficit/hyperactivity disorder. Behav. Res. Ther. 43 (2), 269–276. https://doi.org/10.1016/j.brat.2004.02.002.

Hough, C.M., Luks, T.L., Lai, K., Vigil, O., Guillory, S., Nongpiur, A., Mathews, C.A., 2016. Comparison of brain activation patterns during executive function tasks in hoarding disorder and non-hoarding OCD. Psychiatr. Res. 255, 50–59. https://doi.org/10.1016/j.pscychresns.2016.07.007.

Jenkinson, M., 2003. Fast, automated, N-dimensional phase-unwrapping algorithm. Magn. Reson. Med. 49 (1), 193–197. https://doi.org/10.1002/mrm.10354.

Jenkinson, M., Bannister, P., Brady, M., Smith, S., 2002. Improved optimization for the robust and accurate linear registration and motion correction of brain images. Neuroimage 17 (2), 825–841. https://doi.org/10.1006/nimg.2002.1132.

Jenkinson, M., Beckmann, C.F., Behrens, T.E., Woolrich, M.W., Smith, S.M., 2012. Fsl. Neuroimage 62 (2), 782–790. https://doi.org/10.1016/j.neuroimage.2011.09.015.

Kaiser, R.H., Whitfield-Gabrieli, S., Dillon, D.G., Goer, F., Beltzer, M., Minkel, J., ... Pizzagalli, D.A., 2016. Dynamic resting-state functional connectivity in major depression. Neuropsychopharmacology 41 (7), 1822–1830. https://doi.org/10.1038/npp.2015.352.

Laird, A.R., Fox, P.M., Eickhoff, S.B., Turner, J.A., Ray, K.L., McKay, D.R., Fox, P.T., 2011. Behavioral interpretations of intrinsic connectivity networks. J. Cogn. Neurosci. 23 (12), 4022–4037. https://doi.org/10.1162/jocn_a_00077.

Li, Y.O., Adali, T., Calhoun, V.D., 2007. Estimating the number of independent components for functional magnetic resonance imaging data. Hum. Brain Mapp. 28 (11), 1251–1266. https://doi.org/10.1002/hbm.20359.

Marazziti, D., Consoli, G., Picchetti, M., Carlini, M., Faravelli, L., 2010. Cognitive impairment in major depression. Eur. J. Pharmacol. 626 (1), 83–86. https://doi.org/10.1016/j.ejphar.2009.08.046.

Nakao, T., Nakagawa, A., Yoshiura, T., Nakatani, E., Nabeyama, M., Yoshizato, C., ... Kanba, S., 2005. Brain activation of patients with obsessive-compulsive disorder during neuropsychological and symptom provocation tasks before and after symptom improvement: a functional magnetic resonance imaging study. Biol. Psychiatry 57 (8), 901–910. https://doi.org/10.1016/j.biopsych.2004.12.039.

Pauli, W.M., O'Reilly, R.C., Yarkoni, T., Wager, T.D., 2016. Regional specialization within the human striatum for diverse psychological functions. Proc. Natl. Acad. Sci. U. S. A. 113 (7), 1907–1912. https://doi.org/10.1073/pnas.1507610113.

Poppenk, J., Evensmoen, H.R., Moscovitch, M., Nadel, L., 2013. Long-axis specialization of the human hippocampus. Trends Cognit. Sci. 17 (5), 230–240. https://doi.org/10.1016/j.tics.2013.03.005.

Power, J.D., Barnes, K.A., Snyder, A.Z., Schlaggar, B.L., Petersen, S.E., 2012. Spurious but systematic correlations in functional connectivity MRI networks arise from subject motion. Neuroimage 59 (3), 2142–2154. https://doi.org/10.1016/j.neuroimage.2011.10.018.

Power, J.D., Cohen, A.L., Nelson, S.M., Wig, G.S., Barnes, K.A., Church, J.A., ... Petersen, S.E., 2011. Functional network organization of the human brain. Neuron 72 (4), 665–678. https://doi.org/10.1016/j.neuron.2011.09.006.

Raichle, M.E., 2015. The brain's default mode network. Annu. Rev. Neurosci. 38, 433–447. https://doi.org/10.1146/annurev-neuro-071013-014030.

Raichle, M.E., MacLeod, A.M., Snyder, A.Z., Powers, W.J., Gusnard, D.A., Shulman, G.L., 2001. A default mode of brain function. Proc. Natl. Acad. Sci. U. S. A. 98 (2), 676–682. https://doi.org/10.1073/pnas.98.2.676.

Saxena, S., Brody, A.L., Maidment, K.M., Smith, E.C., Zohrabi, N., Katz, E., ... Baxter Jr., L.R., 2004. Cerebral glucose metabolism in obsessive-compulsive hoarding. Am. J. Psychiatry 161 (6), 1038–1048. https://doi.org/10.1176/appi.ajp.161.6.1038.

Schmithorst, V.J., Holland, S.K., 2004. Comparison of three methods for generating group statistical inferences from independent component analysis of functional magnetic resonance imaging data. J. Magn. Reson. Imaging 19 (3), 365–368. https://doi.org/10.1002/jmri.20009.

Seger, C.A., Cincotta, C.M., 2005. The roles of the caudate nucleus in human classification learning. J. Neurosci. 25 (11), 2941–2951. https://doi.org/10.1523/JNEUROSCI.3401-04.2005.

Shirer, W.R., Ryali, S., Rykhlevskaia, E., Menon, V., Greicius, M.D., 2012. Decoding subject-driven cognitive states with whole-brain connectivity patterns. Cerebr. Cortex 22 (1), 158–165. https://doi.org/10.1093/cercor/bhr099.

Tobia, M.J., Guo, R., Schwarze, U., Boehmer, W., Glascher, J., Finckh, B., Sommer, T., 2014. Neural systems for choice and valuation with counterfactual learning signals. Neuroimage 89, 57–69. https://doi.org/10.1016/j.neuroimage.2013.11.051.

Tolin, D.F., Frost, R.O., Steketee, G., 2010. A brief interview for assessing compulsive hoarding: the Hoarding Rating Scale-Interview. Psychiatr. Res. 178 (1), 147–152. https://doi.org/10.1016/j.psychres.2009.05.001.

Tolin, D.F., Kiehl, K.A., Worhunsky, P., Book, G.A., Maltby, N., 2009. An exploratory study of the neural mechanisms of decision making in compulsive hoarding. Psychol. Med. 39 (2), 325–336. https://doi.org/10.1017/S0033291708003371.

Tolin, D.F., Stevens, M.C., Villavicencio, A.L., Norberg, M.M., Calhoun, V.D., Frost, R.O., Pearlson, G.D., 2012. Neural mechanisms of decision making in hoarding disorder. Arch. Gen. Psychiatr. 69 (8), 832–841. https://doi.org/10.1001/archgenpsychiatry.2011.1980.

Tolin, D.F., Villavicencio, A., 2011. Inattention, but not OCD, predicts the core features of hoarding disorder. Behav. Res. Ther. 49 (2), 120–125. https://doi.org/10.1016/j.brat.2010.12.002.

Tolin, D.F., Witt, S.T., Stevens, M.C., 2014. Hoarding disorder and obsessive-compulsive disorder show different patterns of neural activity during response inhibition. Psychiatr. Res. 221, 142–148. https://doi.org/10.1016/j.pscychresns.2013.11.009.

van den Heuvel, M.P., Hulshoff Pol, H.E., 2010. Exploring the brain network: a review on resting-state fMRI functional connectivity. Eur. Neuropsychopharmacol. 20 (8), 519–534. https://doi.org/10.1016/j.euroneuro.2010.03.008.

Wang, L., Hermens, D.F., Hickie, I.B., Lagopoulos, J., 2012. A systematic review of resting-state functional-MRI studies in major depression. J. Affect. Disord. 142 (1–3), 6–12. https://doi.org/10.1016/j.jad.2012.04.013.

Zhang, S., Li, C.S., 2012. Functional connectivity mapping of the human precuneus by resting state fMRI. Neuroimage 59 (4), 3548–3562. https://doi.org/10.1016/j.neuroimage.2011.11.023.

Zhong, X., Pu, W., Yao, S., 2016. Functional alterations of fronto-limbic circuit and default mode network systems in first-episode, drug-naive patients with major depressive disorder: a meta-analysis of resting-state fMRI data. J. Affect. Disord. 206, 280–286. https://doi.org/10.1016/j.jad.2016.09.005.